Journal Pre-proof

Experimental analysis of operational data for roundabouts through advanced image processing

Marco Bassani, Lorenzo Mussone

Please cite this article as: Bassani, M., Mussone, L., Experimental analysis of operational data for roundabouts through advanced image processing, *Journal of Traffic and Transportation Engineering (English Edition)*, https://doi.org/10.1016/j.jtte.2019.01.005.

1 Original research paper

2

Experimental analysis of operational data for roundabouts through advanced image processing

5 Marco Bassani[a], Lorenzo Mussone[b,*]

6

7 [a] *Department of Environment, Land and Infrastructure Engineering, Politecnico di Torino, Torino 10129, Italy*

8 [b] *Department of Architecture, Built Environment and Construction Engineering, Politecnico di Milano, Milano*

9 *20133, Italy,*

10

Highlights

12 • An investigation carried out to survey vehicle movements at roundabouts was presented.

13 • O/D matrix, classification, trajectories tracking, speed and acceleration from video images

14 analysis.

15 • A number of camera set-up configurations were adopted.

16 • Performance of installation set-ups with different vehicle tracking strategies has been evaluated.

17

Abstract

19 Roundabout is still the focus of several investigations due to the relevant number of variables affecting

20 their operational performances (i.e., capacity, safety, emissions). To develop reliable models,

21 investigations should be supported by devices and related sensors to extract variables of interest (i.e.,

22 flow, speed, gap, lag, follow-up time, vehicle classification and trajectory). Notwithstanding that

23 several sensors and technologies are currently used for data collection, most of them present

24 limitations. The paper presents the investigation carried out to survey vehicle movements at

26   (O/D) matrix, compile a vehicle classification, track individual vehicle trajectories together with

27   corresponding speeds and accelerations along paths. To this end, the authors collected video-

28   sequences that were analyzed with a piece of software developed for that task. To minimize the

29   problems due to perspective distortion, environmental effects, and obstructions, a number of camera

30   set-up configurations were adopted with equipment being placed on central or external poles, and on

31   permanent fixtures such as raised working platforms outside the confines of the intersection area.

32   Performance of those installation set-ups with different vehicle tracking strategies has been evaluated.

33   Particularly, speed has been successfully related to trajectory tortuosity, the result of which

34   emphasizes the tremendous potential of image analysis and opens up to further studies on the

35   evaluation of the operational effects of roundabout geometrics.

36   **Keywords:**

37   Transportation; Roundabout; Image analysis/processing; Vehicle tracking and classification; Operating

38   speed; Trajectory.

39

40

41

42

43   ————————————————

44   * Corresponding author. Tel.: +39 02 2399 5182; fax: +39 022 399 5195.

45   E-mail addresses: marco.bassani@polito.it (M. Bassani), lorenzo.mussone@polimi.it (L. Mussone).

46

47

48

49

50 **1 Introduction**

51 In many countries, roundabouts have increasingly become the intersection of choice due to the

52 positive and acknowledged operational benefits deriving from their geometrics as reported in literature

53 (Curti et al., 2008; Rodegerdts et al., 2010, 2014). Nevertheless, operational performance in terms of

54 capacity, speed, and safety still remains a focus of investigation due to the number of variables, apart

55 from geometric ones, affecting trajectories and speeds of crossing vehicles (Sacchi et al., 2011), and

56 emissions (Fernandes et al., 2015; Salamati et al., 2013).

57 With the objective of developing reliable models, investigations should be conducted using

58 robust tools and with attention being paid contextually to the circulating roadway and all the legs.

59 Such tools have to be able to: (a) extract traffic variables of interest such as flow, speed, gap, lag,

60 follow-up time, vehicle length and weight, as well as vehicle position in time (i.e., vehicular

61 trajectory); (b) ensure that the recording video system is not visible to drivers so as to avoid any

62 behavioural effects; and (c) contribute to a reduction in the resources needed to run the system, also

63 in terms of operator time.

64 Although several sensors and technologies are currently used for traffic data collection in

65 roundabout, most of them are limited in their ability to survey traffic variables, a point which is

66 discussed in the paper. In order to avoid the limitations associated with their use, video recording

67 surveys and related image processing techniques can be successfully employed (Messelodi et al.,

68 2005; Migliore et al., 2006; Mussone et al., 2013).

69 The paper proposes a methodological contribution to analyse speed and trajectories of vehicles

70 through roundabouts. It presents the activities undertaken by the authors in the development and use

71 of a video recording system in conjunction with a software developed for the derivation of: (a) the

72 origin/destination (O/D) flow matrix, (b) the vehicle classification, and (c) the trajectories and

73 associated speeds and curvature diagrams along the paths traversing a roundabout.

75   ## 2 Background

76   ### 2.1 Vehicle position data collection tools

77   At present, many multi-purpose detectors for traffic data collection are available at affordable prices.

78   Laser, radar, microwaves, infrared, acoustic, ultrasonic, capacitive, piezoelectric, magnetometric, and

79   magnetic loops are the technologies employed in sensors. With more or less similar levels of

80   efficiency and precision, all the above-mentioned technologies allow for the collection of macroscopic

81   variables such as flow, speed, density (or occupancy) and vehicle specific variables such as headway,

82   gap, lag, follow-up time and vehicle length and weight.

83   Their main disadvantage (apart from the fact that they sometimes need to be physically supported

84   or that, in some cases, their installation can occasionally lead to an intrusion into the traffic circulation

85   area) is that their measurements refer to a single road section or linear segment, and therefore

86   multiple measurement points require an array of collection tools. None of them, in fact, may be

87   employed for vehicle tracking, especially in situations where vehicles move along inflected trajectories

88   (e.g., in case of roundabouts). This would not be a serious problem unless it is strictly necessary that

89   information gathered by detectors relates uniquely to each individual vehicle. This task is particularly

90   crucial at roundabouts where the construction of the O/D matrix is very challenging (Grenard and Wei,

91   2012).

92   One possible way to track vehicles could be the floating car data method that, however, requires

93   that a statistically significant number of vehicles are equipped with positioning sensors i.e., global

94   positioning system-global navigation satellite system (GPS-GNSS), inertial measuring unit (IMU) or

95   combined sensors, with data recorded on board and/or transferred to a central system. With this

96   method, installations and experiments are expensive and complicated since it (the method) needs a

97   large number of vehicles together with the participation of the general public to be of any use in a

98   realistic setting. However, the current wide diffusion of navigation systems working in real time and

99   connected to a central unit makes this feature of increasing interest for the near future, at least for

102   collection of clouds of data and could be used to track vehicles. At present, however, they are more

103   expensive than video-image technology and entail a higher level of complexity and effort in the

104   collection and modelling of a large quantity of data.

105   Consequently, the most promising methodology available at present for the tracking of vehicles is

106   certainly represented by the video analysis technique. Several contributions have demonstrated that it

107   may be employed in a variety of applications from simple vehicle detection (Messelodi et al., 2005;

108   Wei et al., 2005) to the gathering of comprehensive data for trajectories in both time and space

109   domains, thus allowing a complete reconstruction of movements along sections (Beymer et al., 1997)

110   and at vehicle intersections (Alhajyaseen et al., 2013; Apeltauer et al., 2015; Datondji et al., 2016;

111   Dinh and Tang, 2017; St-Aubin et al., 2013) or cyclist behaviour trajectory analysis (Sakshaug et al.,

112   2010; Zaki et al., 2013).

113   With the aim of providing information useful for the calibration of microscopic simulation models,

114   Alhajyaseen et al. (2013) analysed the relationship between speed and trajectory at at-grade urban

115   intersections. Adopting the survey technique described in Suzuki and Nakamura (2006), those authors

116   demonstrated the effect on vehicle trajectory of geometry (angles between legs, corner radii, number

117   of exit lanes, and positions of hard noses of the medians) for different vehicle types negotiating the

118   intersection at different speeds, confirming the potential of the image analysis technique when

119   conducting surveys to gather positioning data at road junctions. In Mussone (2013), the question of

120   visibility on roundabouts was faced by using real trajectories extracted from video image records.

121   Finally, the possibility to track vehicles in roundabouts by video cameras mounted on drones has

122   raised a certain interest. Guido et al. (2016) used them to detect and compare tracking data with GPS-

123   equipped vehicles only. According to the authors, the methodology is promising but needs to be

124   improved for removing noise and inaccuracies due to uncontrolled movements and vibrations of

125   drones under the effects of wind.

126   *2.2   Position and speed data modelling at roundabouts*

129 103 US roundabouts with geometric, operational, and safety data was carried out (Rodegerdts et al.,

130 2007). Of these, 31 roundabouts were the focus of video recordings in the spring and summer of 2003,

131 with 34 h of traffic operation data accumulated (i.e., flow measurements, gaps, delays and travel times,

132 turning movement proportions, and vehicle types). For this purpose, a video recording system

133 consisting of analogic and digital video cameras was used. Operational data were recorded making

134 use of "event recording" software (Rodegerdts et al., 2006). In the same study, sixteen single-lane and

135 eleven multi-lane roundabouts were considered for the operating speed surveys (Fig. 1).

136   In Rodegerdts et al. (2007), speed data were collected through the use of radar guns only at four

137 specific locations: one outside (i.e., at 60 m from the yield line) and three inside the roundabouts. In

138 particular, as seen in Fig. 1, they were collected at the yield line (section 1), at the midpoint of the

139 adjacent splitter island (section 2), and at the exit (section 3), with a minimum number of speed data

140 per section greater than 30 to achieve a statistical significance. Speed data collected at the

141 roundabouts were differentiated both by movement type (i.e., left, through or right turn), and by vehicle

142 type (i.e., passenger cars, trucks), and only passenger car data were used for that analysis.

143
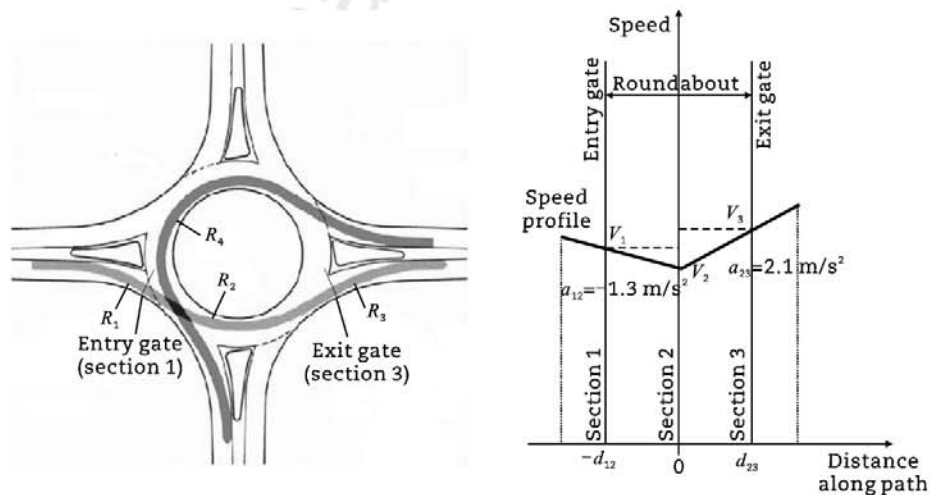
144
145 **Fig. 1** Layout of the operating speed surveys (Rodegerdts et al., 2010). (a) Geometric characteristics of trajectories. (b) Schematic speed profile.
146

147   Starting from the elementary arc with the minimum radius on which the minimum speed is reached

148 in the circulatory roadway (V_2), speeds at the entry (V_1) and exit (V_3) gates can be derived under the

149 hypothesis of naturally decelerated/accelerated motion and adopting average deceleration (a_{12}) and

150 acceleration (a_{23}) values from observational data (Robinson et al., 2000).

151   The predictive speed equations (Rodegerdts et al., 2007) for the through movement for entry (V_1)

152 and exit (V_3) speeds in km/h (Fig. 1) are

153
$$V_1 = \min\left\{ V_{1\text{base}}; 3.6\sqrt{\left(\frac{V_2}{3.6}\right)^2 - 2a_{12}d_{12}} \right\} \tag{1}$$

154
$$V_3 = \min\left\{ V_{3\text{base}}; 3.6\sqrt{\left(\frac{V_2}{3.6}\right)^2 + 2a_{23}d_{23}} \right\} \tag{2}$$

155 where a_{12} is the deceleration between the point of interest of the entry path and the midpoint of the

156 path (assumed equal to -1.3 m/s^2), a_{23} is the acceleration between the midpoint of the path and the

157 point of interest of the exit path (assumed equal to 2.1 m/s^2), and d_{12} and d_{23} are the distances

158 between the points of interest along the entry and exit paths, and the midpoints of these paths

159 respectively, which are measured along the vehicle trajectory. In Eqs. (1) and (2), $V_{1\text{base}}$, V_2 and $V_{3\text{base}}$

160 represent the predicted speeds at the entry, midpoint and exit points based on path radii R_1, R_2 and R_3

161 (Fig. 1) using the basic formula of vehicle equilibrium on curves (Eq. (3)).

162
$$\begin{cases} V_{1\text{base}} = \sqrt{gR_1(f+q)} \\ V_2 = \sqrt{gR_2(f+q)} \\ V_{3\text{base}} = \sqrt{gR_3(f+q)} \end{cases} \tag{3}$$

163 where g is the acceleration of gravity (equal to 9.81 m/s^2), f is the side friction factor, and q is the

164 super-elevation, which is normally -2% in the case of modern roundabouts (Rodegerdts et al., 2007).

165 Eq. (3) may also be used to evaluate the speed along a left turn movement, using the value of R_4

166 indicated in Fig. 1 as a radius.

167   A comparison between the 85th percentile speed observed in the field and the corresponding

168 values predicted using Eqs. (1) and (2) demonstrated that the proposed model was applicable to

169 those maneuvers in which vehicles interact with the central island (left turn and through movements),

170 and that it was considered conservative because it tends to overestimate the operating speed. The

173 prediction of speed on the circulatory roadway. This leads to the conclusion that the evaluation of

174 operating speed at roundabouts still remains a challenge at both the analysis level and design stage

175 (Šurdonja et al., 2018; Perco et al., 2012).

176 Currently, TORUS (Transoftsolutions, 2018) and CIVIL 3D (Autodesk, 2018) software packages

177 consider the fastest path analysis according to literature (Robinson et al., 2000; Rodegerdts et al.,

178 2007). These programs calculate the expected speed on the circulatory roadway along the minimum

179 radius along the "fastest vehicle path", which represents the smoothest possible trajectory of a vehicle,

180 in the absence of other vehicles and ignoring all lane markings, from the entry to the exit gates (Ahac

181 et al., 2016; Rodegerdts et al., 2006).

182 **3 Methodology**

183 Starting from this literature review, the authors proposed a comprehensive methodology to collect

184 video records from existing roundabouts and derive information useful to model the relationship

185 between speeds and trajectories of vehicles. The tracking of trajectories gives also the possibility for

186 the derivation of trajectory tortuosity parameters, as well as the reconstruction of O/D matrix. From the

187 length of moving objects in the road scene, a neural network was trained to classify vehicles along

188 each movement.

189 To minimize the problems due to perspective distortion, environmental effects, and obstructions, a

190 number of camera configurations were adopted with equipment being placed on central or external

191 poles (with respect to central island), or on permanent fixtures such as raised working platforms

192 outside the confines of the intersection area. Strengths and weaknesses of the selected installations

193 are described in order to determine the optimal set-up. Three case studies in Northern Italy were

194 considered. Up to three video cameras were used in different set-ups. Each installation exhibited a

195 different behaviour under the effects of wind, cloud cover, shadows, dazzle, perspective deformation,

196 and obstructions. Two additional aspects, namely ease of perspective correction and synchronization

197 between video cameras, were also investigated and solved.

200 task is easier when cameras are mounted on the same pole and camera output can be connected

201 directly to the same computer. More demanding is the case when several cameras on different poles

202 are involved and a wireless connection is needed to link the computers together to use the same

203 timestamp. Besides this, the authors experimented two different strategies in order to build trajectories:

204 by merging trajectories extracted by separated images (MT) and blending images before extracting

205 trajectories (BI).

206   Finally, the data collected from image analysis in the three case studies have provided general

207 relationships between speeds and trajectories as affected by roundabout geometrics. Differently from

208 the approach of Robinson et al. (2000) and Rodegerdts et al. (2007), continuous speed and trajectory

209 data help the authors in the development of a new model able to relate speeds to trajectory tortuosity.

210 The possibility to work out such a model can be considered by analysts and designers as an

211 opportunity to predict speed behaviour of drivers along their path on the basis of roundabout

212 geometrics.

213 *3.1   Survey tools and methodology*

214 The instrumentation used to collect and evaluate data consists of a vision system and a real time

215 kinematics-global positioning system (RTK-GPS), both connected to a dedicated PC (Fig. 2). In

216 Mussone et al. (2011, 2013), a more detailed description of the system, including details of both

217 hardware and software characteristics, can be found. Images from video cameras must not have blind

218 spots and this condition can be achieved through a planned set up of optics and video camera

219 orientation.

220   The vision system (Fig. 2(a)) consists of one to three cameras with a resolution of 1360 x 1024

221 pixels. The optical lens of each video camera was adjusted in line with the application scenario by

222 remote control. The vision system provided information on vehicular flow through the processing of

223 images recorded by the video camera(s), while the RTK-GPS system was used to generate data

224 useful for calibrating and evaluating the vision system.

227 Trimble Zephyr Antenna, is attached to a probe vehicle and connected via radio link (DiGi XBee Pro

228 modules in point to point mode) to the base station.

229

230 (a) (b)

231

232 **Fig. 2** Data collection and evaluation instrumentation. (a) Vision system placed upon a raised working platform. (b) The probe vehicle

233 with the rover system.

234

235 In order to improve the process of matching video camera data with GPS data, a series of marked

236 points visible in video images were drawn on the pavement surface of the roundabout (four points on

237 each leg, and from four to eight points on the circulatory roadway depending on the dimension(s) of

238 the central island). The exact positions of these points were, then, attained by both GPS (with an

239 accuracy ranging from 2 to 15 cm) and by video recording. The matching of vehicle coordinates (and

240 then speed) data calculated by image processing with the data gathered by GPS was then a relatively

241 straightforward task.

242 Calibration of the vision system was carried out for image rectification, thus tuning the Bouguet

243 camera model of the vision system. Image rectification aims at achieving homogeneity in terms of

244 corresponding pixels in the image plane, and the ratio between lines lengths and angles in a specific

245 plane of the observed world (i.e., the central islands is circular but it appears an ellipse in the

246 perspective projection). This requires a proper image transformation, i.e., a homography between the

248   effective and more accurate than when carried out on the original image. The homography is known

249   when the size and the position of some specific elements of the observed scene are available.

250   *3.2   Pre processing*

251   The images gathered require conversion, undistortion, and rectification, while RTK-GPS data need

252   data conversion (for rover data) and synchronization between base station and rover timestamps.

253   The image analysis was carried out by a software (developed at Politecnico di Milano and based on

254   MATLAB platform) named Vehicle Tracking for Roundabout Analysis (VeTRA), which employs genetic

255   algorithm optimization procedures to minimize the re-projection error of the central island onto the

256   image plane, and also provides a complete projective transformation from the 3D real world to the 2D

257   image, by constraining world points to lie at ground level.

258   The current version of VeTRA has further improved performance in blob recognition with respect to

259   the original version used in Mussone et al. (2011). Improvements to the algorithms have now limited

260   the negative effects of some environmental factors (i.e., wind, sudden changes in light conditions due

261   to clouds), occlusions due to fixed objects (i.e., trees, poles) and moving vehicles (Oh et al., 2012), as

262   well as perspective deformations.

263   The key tool in VeTRA is its tracking system, which detects moving objects in the field through an

264   adaptive background modelling and subtraction algorithm. The image areas representing the vehicles

265   (known as "blobs" in information science jargon) are identified in the foreground through shadow and

266   noise removal. The tracking system is capable of distinguishing between newly detected blobs and

267   previously tracked vehicles between three types of vehicles as explained in the next paragraph. The

268   blobs are continuously updated as new information is received. All these activities rely on a proper

269   model of the background, which has to be sufficiently robust to contend with daily changes in light

270   conditions and camera oscillations. Although the tracking system detects the movements of objects in

271   the background, it is able to filter and hence exclude from computation all the small movements of any

272   objects (i.e., trees, sheets on the pavement, etc.) affected by wind.

275   (here called Merging Trajectory (MT) strategy), the second blends images from video cameras before

276   extracting trajectories from the blended images (here called Blend Images (BI) strategy). There are a

277   number of problems and advantages associated with each strategy that were tested in this experiment.

278   With the MT strategy, the trajectory of the same vehicle is extracted from video cameras (two or

279   more) as in the approach with one camera only. After that, trajectories of the same vehicle are

280   associated and superimposed in order to obtain only one trajectory. The challenging activity is the

281   association of trajectories avoiding strong discontinuities between them.

282   With the BI strategy, a new image is generated from the blending of all images collected to exclude

283   the portions of images affected by distortion. Then, blended images are analysed as in the one

284   camera approach to extract trajectories.

285   The MT strategy makes it easier to extract blob trajectories separately from each video camera but

286   does not guarantee a perfect continuum (in the sense of function derivability) of single trajectories. On

287   the other hand, the BI strategy allows a final complete trajectory which is perfectly continuous but

288   requires considerable effort due to merging images. In fact, isomorphic transformation and

289   perspective correction must be applied to each image to maintain the same scale over the trajectory.

290   It is worth noting that new set-ups with a different number of video cameras required an

291   improvement of the original version of VeTRA (Mussone et al., 2013). The new images produced by

292   blending separate images, or the new trajectories derived from mixing the trajectories given by each

293   video camera, are significant results for the post processing phase.

294   *3.3   Post processing I – trajectory reconstruction*

295   For each video survey, the blob trajectories produced by the tracking system are processed and

296   stored in a database in order to generate the O/D matrix, vehicle trajectories, speed profiles and the

297   vehicle classification.

298   Trajectories on pavement surfaces are calculated from trajectories between the entry and exit gates

299   of the circulatory roadway on the image plane using RTK-GPS data collected by the rover on the

302   then saved to a system of local coordinates. Speed and curvature profiles are obtained from

303   calculations based on vehicle position and time. Speed is calculated for two consecutive points by

304   simply dividing the distance between them by the elapsed time (equal to the frame rate of the camera,

305   except in those very rare cases where some frames have been lost).

306   The tracking system used in VeTRA follows two different procedures. The first one is less

307   sophisticated and is employed for flow classification purposes as it distinguishes between (a) bikes

308   and motorbikes, (b) light vehicles, vans and campers, and (c) heavy vehicles. It detects the blob for

309   each vehicle, which is then tracked from the entry to the exit section. In this paper, only classes (b)

310   and (c) were used for performance comparison since too few bikes and motorbikes were observed

311   during the survey.

312   Classification is based on vehicle dimension, particularly on its length, which is derived from blob

313   length. Since blob dimension generally changes according to its position inside the image (that is, the

314   position inside the circulatory roadway) due to perspective distortion, a neural network (NN) was used

315   to classify vehicle length by using for training some images sampled from vehicle trajectory,

316   accurately divided by movements. The NN must be trained in every location because it needs to learn

317   the effect of perspective distortion along the circulatory roadway. The accuracy of NN recognition was

318   high with an error lower than 3% for trajectories closer to video camera; higher errors were observed

319   for short trajectories, and for those farther from the video camera where perspective distortions may

320   create difficulties in recognition.

321   The second tracking procedure is more accurate and is employed for trajectory and speed analysis.

322   It recognizes the barycentre (or centroid) of each blob in 2D and produces a continuous curve formed

323   by points that are known in the space and time domains. More details on tracking procedures are

324   available in Mussone et al. (2013).

325   *3.4 Post processing II – data treatment for speed analysis*

326   A filtering algorithm in VeTRA was included to reject trajectories in which the speeds are too low due

329 ones were excluded from the speed analysis to obtain free flow speeds only. As a result, trajectories

330 with average speeds between entry and exit lower than 10 km/h were discarded. Filtering was also

331 necessary to exclude stationary vehicles in the circulating roadway, or affected in trajectory by

332 conflicting vehicles. In fact, in some cases, very low speeds were the result of superimposition of

333 trajectories (and blobs) of two or more vehicles.

334   When available in time and space domains, the trajectory of any isolated vehicle traversing the

335 roundabout in free-flow conditions contains all the information necessary for an assessment of how

336 the said vehicle trajectory was affected by the geometry of the roundabout. Tortuosity indexes may be

337 used to characterize curved trajectories. In this paper, two tortuosity indexes, having as an objective

338 the characterization of the vehicle paths associated with specific maneuvers (crossing, right, left and

339 U-turn), have been derived by reference to general literature. It is obvious that these indexes cannot

340 capture all aspects of driver behaviour but they are helpful in understanding whether the trajectory

341 itself and related vehicular speed are confined to a range within recommended operating intervals.

342   According to Fig. 3, the first index (T_1) (a derivation of index T_2, presented hereafter) is shown as

343 follow

$$T_1 = \Sigma_i \left(|\alpha_i|/R_i\right)/L \tag{4}$$

345 where $|\alpha_i|$ is the absolute value of the angle between the tangents passing from two successive

346 recorded points (P_i and P_{i+1}, P_{i+1} and P_{i+2}), R_i is the radius of the osculating circle that is derived from

347 thirty points around the considered one (15 before $-P_{i-15}$, $\cdots$, P_i, and 15 after $-P_{i+1}$, $\cdots$, P_{i+15}), L is the

348 length of the trajectory between the entry and the exit gates, and i is one of the considered points. The

349 sum over i includes all the points between the entry and the exit gates. Thirty-one points allow to

350 manage a set of images of one second duration (at the current frame rate), which can be considered

351 long enough to smooth peaks due to random noise effects in blobs.

352   The second tortuosity index (T_2) is obtained with the Eq. (5).

$$T_2 = \Sigma_i \left(|\alpha_i|/L\right) \tag{5}$$

354   Eq. (5) is also known in literature as the curvature change ratio (Yasser and Mohamed, 2011)
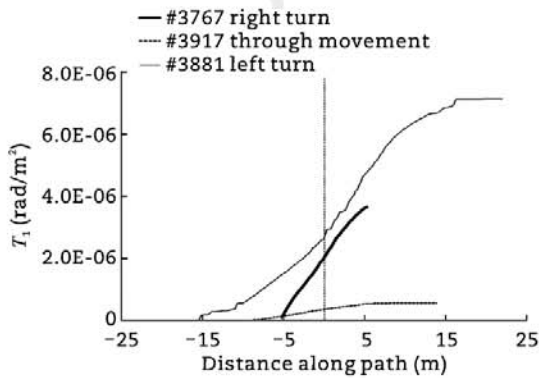
356   (a)
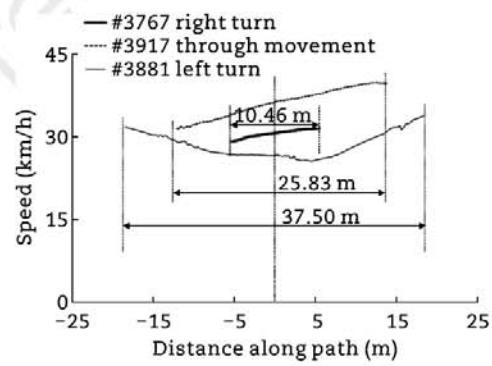

357

358   (b)

(c)

359

360   (d)
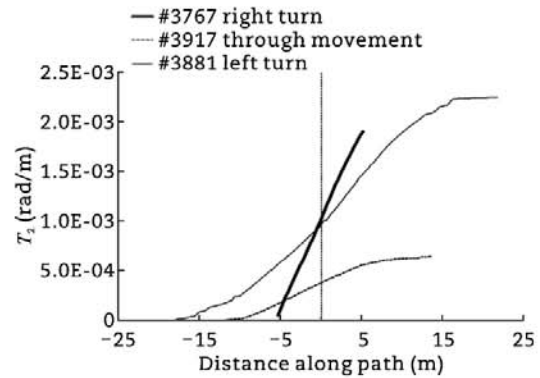

(e)
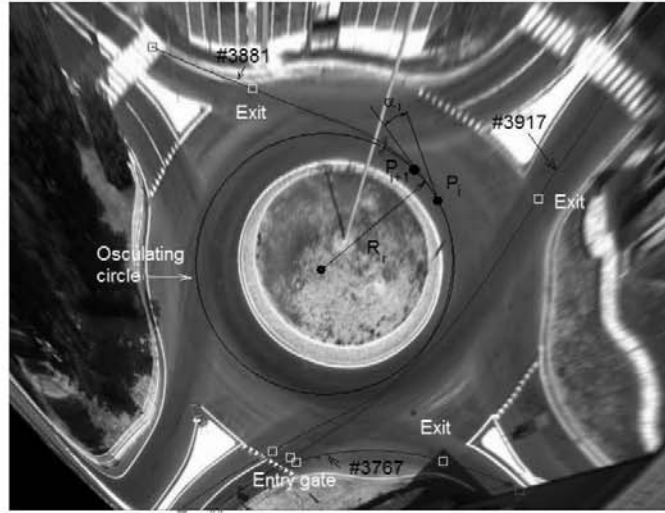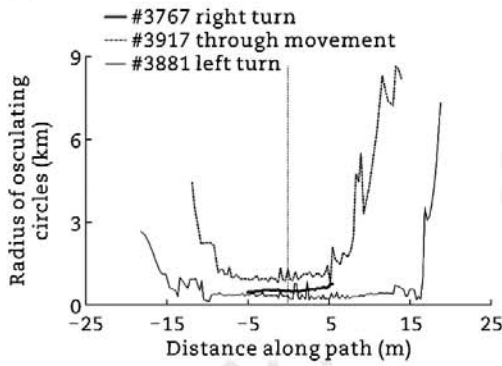
361
362
363   **Fig. 3** Trajectory analysis. (a) Typical curves for parameter analysis. (b) Trajectory radius. (c) Speed. (d) T_1. (e)
364   T_2.
365   Fig. 3 shows the typical curves for the four parameters extracted from trajectory analysis (trajectory

367   turn was not considered due to the paucity of data examples). In the same Fig. 3, the cumulated

368   values of these two indexes from the initial point at the entry gate (i = 1) to the generic points (i) along

369   the trajectory is also plotted.

370   The two indexes indicate the level of difficulty in negotiating the roundabout, which is higher when

371   the angles are high and the corresponding radii are small. The units of measurement for the two

372   tortuosity indexes are rad/m^2 and rad/m, respectively. In Fig. 3(d) and (e), they have been plotted

373   according to the formulas with values that increase along the travelled path, for three trajectories

374   selected from the Biella roundabout database (each identified with a 4-digit code). In Fig. 3(b) and (c),

375   for the same three trajectories, the radius of the osculating circles and the speed profile are plotted. It

376   is worth noting that in Fig. 3, the central point of the path has a reference station equal to 0.

377   As previously indicated, the speed at each of the P_i points along a generic trajectory is calculated by

378   simply dividing the distance between every point P_i and the consecutive point P_{i+1} by the elapsed time

379   (equal to the frame rate of the video camera that was equal to 0.0333 s). For the radius diagram,

380   thirty-one consecutive points of the trajectory (resulting in 1 s of images) have been considered for the

381   estimation of R_i values.

382   **4   Investigation**

383   With a view to establishing the optimal camera configuration and assessing the performance of

384   VeTRA, in-field research activities were initially undertaken at five roundabouts in northern Italy

385   (Piedmont and Lombardy regions), chosen for their geometrical characteristics and environment (rural

386   and urban). Table 1 reports a synthesis of the geometric characteristics and the most significant

387   survey data, while Fig. 4 illustrates three general video camera configurations used for the surveys.

388   Unfortunately, two other sites with different set-ups and in urban environment were investigated but

389   recorded images were unusable due to the effects of a strong wind in one case and to a reflected

390   dazzle in the latter that were not possible to remove.

391   Images were recorded for between 1.5 and 2 h to obtain at least one hour of actual flow. The

394   The first roundabout is located near the urban limits of the city of Biella (Fig. 5, with the identification

395   of tracked vehicles, entry and exit gates, and video camera direction (arrow)), and connects two

396   arterials with two lanes per direction and separated carriageways.

397   Pedestrian crossings are provided at three of the four legs. The external diameter is 50 m, the

398   circulatory roadway is 13 m in width, while the central island diameter is equal to 24 m including a

399   truck apron of 1.5 m. The approaching legs have two lanes with an average width of 8 m, while 6 m is

400   the width of the single lane departure legs. The roundabout is equipped with a lighting tower headlight,

401   while the water harvesting systems are located outside the circulatory roadway. During the study, the

402   detection system was placed on a moveable rack near the edge of the southwest corner. The video

403   camera, pointing towards the centre of the roundabout, was placed at a height of about 22 m at an

404   angle of approximately 55° with respect to the rack axis.

405
406

Table 1 Synthesis of information for survey activities.

Roundabout	Biella	Ghisalba	Poncarale
Latitude	45°33'12".39	45°35'32".21	45°27'29".99
Longitude	8°04'21".85	9°46'19".75	10°12'09".66
Inscribed diameter, D_{INS} (m)	50	46	70
Inner island diameter, D_{INT} (m)	24	26	56
Circulatory roadway width, W_{CR} (m)	13	10	7
Number of legs	4	4	4
Configuration # (Fig. 4)	1	2	3
Number of cameras	1	3	3
Manufacturer	Goyo GM12314S	No.2 Goyo GM12314S (2.30 mm, 94°)	Goyo GM12314S
(focal length, FOV)	(2.30 mm, 94°)	No.1 Theia MY125M (1.43 mm, 125°)	(2.30 mm, 94°)
Number of survey points	1	1	2
Video camera position	External	Internal	External
Horizontal angle (°)	-	90	120
Vertical angle (°)	55	40	72 (1 camera)
			55 (2 cameras)
Camera height (m)	22	22	32

407   Note: FOV is field of view

410 (a)
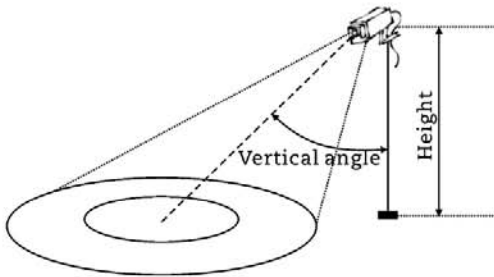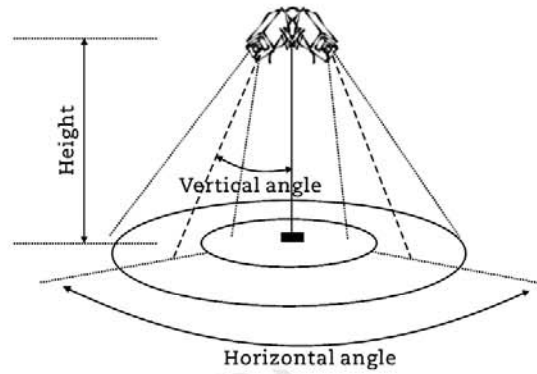
411
412
413 (c)
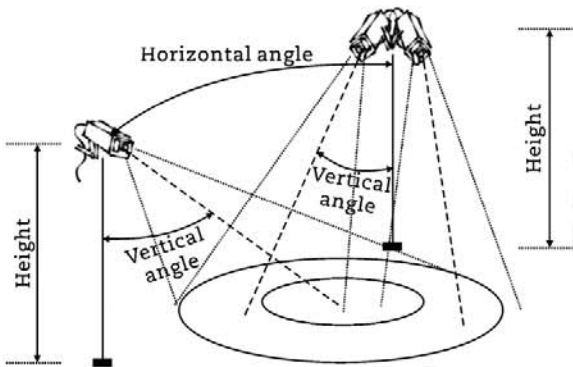
414
415 **Fig. 4** Scheme of the three video camera configurations adopted for the survey. (a) Configuration #1. (b) Configuration #2. (c)
416 Configuration #3.
417

418

421   The second roundabout is located in a rural area near Ghisalba (Fig. 6(a)) at the intersection of two

422   single-carriageway rural highways with no pedestrian crossings. The external diameter is 46 m, the

423   circulatory roadway is 10 m, and the central island diameter is equal to 26 m with a truck apron of 2 m.

424   The roundabout is furnished with a central lighting tower headlight. The detection system, consisting

425   of three cameras, was placed on the lighting pole in the centre of the central island at a height of

426   about 21 m above the roundabout plane, with the three cameras facing east, north and west

427   respectively and placed at vertical angles of approximately 40° with respect to the pole.

428   The third roundabout lies outside the urban area of Poncarale (Fig. 6(b)) at the intersection of two

429   main highways, both of which are single carriageway with two-way traffic and no pedestrian crossings.

430   The external diameter is equal to 70 m and the circulatory roadway is only 7 m. As a result, the

431   roundabout has a wide central island (56 m in diameter) that includes a truck apron of 2.5 m. In

432   contrast with the other two roundabouts, the approaching and departure legs of the Poncarale

433   roundabout are tangent to the circulatory roadway. The lighting is provided by two lighting towers,

434   located on two divisional islands to the north and south, distant 81 and 28 m respectively from the

435   roundabout.

436   (a)   (b)
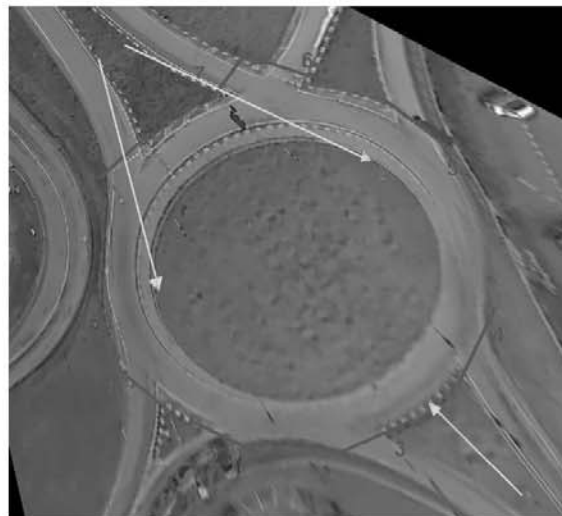
437
438   **Fig. 6** Aerial view of roundabouts. (a) Ghisalba roundabout. (b) Poncarale roundabout. (Arrows indicate video-camera direction).

439   The measurements were taken with three cameras installed at a height of 32 m, two of which were

441 lighting pole at an angle of approximately 72°. The cameras were attached to the lifting system to

442 which the lamps of the central pole are fixed. This system is lifted and lowered whenever lamp

443 maintenance is conducted. Since the video cameras were close to the lamps, it is reasonable to

444 assume that they were not seen by drivers and so did not influence their behaviour. Survey vantage

445 points were determined according to the particular set-up adopted (Fig. 4), with video cameras able to

446 cover the entire roundabout.

447 **5   Results and analysis**

448 *5.1   Vehicle classification and O/D matrix*

449 As explained before, the classification of vehicles has been limited to two classes of vehicles (light

450 and heavy) which, when combined, represent more than 95% of the total observed flow for the three

451 investigated case studies. Classification is worked out by a neural network previously trained through

452 a sample of cases which are manually extracted.

453 Using different combinations of the two strategies cited previously (merged trajectories (MT) and

454 blended images (BI)), the number of video cameras (from one to three (1C–3C)) and configurations

455 (from #1 to #3), five different cases have been considered and reported in Table 2 to validate the

456 estimates produced by VeTRA. In Table 2, the results are shown for all the possible sixteen

457 movements into a 4-leg roundabout, with the last row containing the total number of movements

458 recorded by VeTRA and the corresponding average values counted by the operators (specifically,

459 three people who manually counted vehicles looking at the videos and subdividing such counts by

460 movements).

461 The data elaborated by VeTRA and expressed in percentage terms (v_i), calculated on the total

462 collected flow, were compared with those obtained from video observation by a number of operators.

463 These measurements are reported in Table 2 in percentage under the column "Operator" (o_i), and

464 were repeated until the average values between observations were significantly stable (i.e., the mean

465 did not change anymore with the addition of new observations, according to the central limit theorem).

467 repeated extractions (analysis of same video images by the same operator) lead to a reduction in

468 error when estimating the mean. It should be noted that the total number of vehicles observed in one

469 hour of survey time was high (1500–2500 veh/h).

470
471 **Table 2** Comparison of percentage values of the O/D matrixes for Biella, Ghisalba and Poncarale roundabouts.

O/D movement	Biella (configuration #1)		Ghisalba (configuration #2)			Poncarale (configuration #3)		
	Operator (%)	VeTRA (%) 1C	Operator (%)	VeTRA (%) 3C-MT	3C-BI	Operator (%)	VeTRA (%) 1C	2C-BI
2-1	0.40	0.59	0.00	0.00	0.00	0.14	0.00	0.10
2-3	2.93	3.37	2.98	4.72	3.56	7.14	4.70	12.02
2-5	20.96	20.33	26.46	23.29	25.89	7.24	3.65	0.10
2-7	0.47	0.44	1.08	1.15	1.47	3.48	1.05	6.11
4-1	3.26	2.49	0.00	0.00	0.00	5.43	5.89	7.46
4-3	0.20	0.26	0.00	0.10	0.05	0.28	0.07	0.10
4-5	4.64	4.80	0.66	1.20	0.95	4.64	7.36	0.10
4-7	7.82	6.87	2.53	2.45	2.61	17.76	18.58	30.05
6-1	19.79	21.13	0.00	0.00	0.00	9.60	12.90	0.00
6-3	4.66	2.60	0.00	0.14	0.00	4.08	4.84	0.00
6-5	0.29	0.00	0.00	0.05	0.00	0.09	0.07	0.00
6-7	7.07	8.68	31.22	30.46	29.98	0.19	0.84	0.21
8-1	2.05	2.71	30.60	31.95	31.54	7.79	8.27	9.12
8-3	11.90	13.27	2.03	2.26	2.19	19.67	27.70	34.09
8-5	13.22	12.24	2.40	2.17	1.71	12.29	3.86	0.00
8-7	0.33	0.23	0.04	0.05	0.05	0.19	0.21	0.52
Total flow (veh)	2002	2060	2415	2078	2105	2156	1706	1154

472

473 In this phase, the authors focused mainly on error evaluation rather than on absolute values, so

474 Table 2 reports the percentage values for each movement with respect to the total number of

475 movements.

476 Bernardin and Stiefelhagen (2008) suggested the use of clear multiple object tracking (MOT)

477 metrics to measure the performance of video image processing. It is made up of two indexes: (a) the

478 total error value averaged by the number of matches made when estimating position (indicated as

479 MOTP–multiple object tracking precision–and discussed in the next subparagraph), and (b) the

480 tracking accuracy (MOTA–multiple object tracking accuracy), estimated using the following equation.

482   where for any time t, m_t is the number of misses, fp_t is the number of false positives, mmc_t is the

483   number of mismatches, and g_t is the number of objects.

484   In this application, we calculated MOTA using all data collected by operator but only data for

485   completely detected trajectories by VeTRA (since partially revealed trajectories are not of interest in

486   this context and then the number of objects, g, is lower), thus leading to possible worse performance.

487   Therefore, the subscript t (usually the index of each frame) is here assumed to be linked to a whole

488   trajectory. This index varies from 1 to 0 (from best to worst performance). Besides, differences

489   between operator and VeTRA are firstly calculated for each movement and then summed up. Three

490   other different error types were also calculated from Table 2 and listed in Table 3 according to

491   performance indexes used in technical literature: the sum of absolute differences (E_1), the average of

492   absolute differences (E_2), and the average of differences (E_3). E_1, E_2, and E_3 are calculated according

493   to the following equations.

494
$$E_1 = \sum_i |v_i - o_i| \tag{7}$$

495
$$E_2 = \sum_i |v_i - o_i|/n \tag{8}$$

496
$$E_3 = \sum_i (v_i - o_i)/n \tag{9}$$

497   where n represents the number of movements considered in the analysis.

498   Difference between E_1 and E_2 depends only on the number of movements n taken into

499   consideration but this number may change from site to site. Hence, when comparing performance of

500   two sites, it may be useful to use both indexes. Besides the indexes, their percentages were also

501   taken into consideration. They were calculated considering $v_i / \sum_i v_i$ instead of v_i for E_1, and

502    $o_i / \sum_i o_i$ instead of o_i for E_2. For E_3, the average percentage is always nil.

503   It must be stressed that operators represent the way to obtain the true result by application of the

504   central limit theorem. In this experiment, since an infinite number of operators is not possible, the

505   calculated averages may be considered a good estimate of the true result. VeTRA results are,

506   nonetheless, affected by deterministic errors that cannot be completely avoided since they are

507   intrinsic to the system (i.e., video cameras and lenses).

508   Values for the average of the absolute differences (Table 2) between operator and VeTRA

509   generated data are less than 5% and are compatible with traffic analysis resolution. This also holds

511   In contrast, the sum of percentage differences is generally very high even with the best strategy (see

512   Ghisalba-Bl and Biella-1C in Table 2).

513   This last result shows the existence of a bias due to the general set-up conditions during the survey.

514   The fact that bias is positive indicates that VeTRA has generally estimated a lower percentage value

515   for each movement than that obtained by the operators. In the cases of Biella and Poncarale, the bias

516   is positive, while in Ghisalba, it is negative.

517   On examination of the five analyses carried out with VeTRA (Tables 2 and 3), the best results were

518   obtained with configuration #1 in Fig. 4, in particular when considering the MOTA index. In fact, the

519   performance obtained with the use of one video camera, which has lower costs and requires less

520   effort, is quite similar to that of configuration #2 in which three video cameras are employed. Moreover,

521   in the latter case at least four video cameras would be necessary to ensure adequate coverage of the

522   entire surface of the roundabout (Fig. 6).

523   The problems resulting from the blending of sequences obtained from three video cameras located

524   at 32 m from the roundabout (configuration #3 of Fig. 4) led to the necessity of considering two

525   different strategies in the analysis of the Poncarale roundabout. Although the performance indicators

526   (in Table 3) in the case of three-camera (Ghisalba-3C) and also a single camera (1C) configurations

527   are still quite close to those established in the Biella case study, the use of a two-camera (2C)

528   configuration with blended images results in the worst performance observed.

529   The use of additional cameras can result in operating problems related to factors such as

530   synchronization between frames from different cameras, different orientations and separated

531   communication wires. Synchronization is an acute problem that can be exacerbated by the loss of

532   some frames. In addition, the different orientation of video cameras requires different isomorphisms,

533   that is, different camera calibrations and homography transformations. The result obtained for E_3 of

534   Biella, which is indeed very low, is not surprising since Eq. (9) does not use absolute values and

535   therefore errors, which are not very biased in this case, cancel each other.

536

539
540

Table 3 Performance indicators (errors) between operator and VeTRA computed values according to Eqs. (6)-(8).

Roundabout and image treatment strategy	E_1 (sum of absolute differences)		E_2 (average of absolute differences)		E_3 (average of differences)	MOTA (%)
	Percentage (%)	Value (veh)	Percentage (%)	Value (veh)	Value (veh)	
Biella (1C)	11.64	58	0.72	4	0.89	88
Ghisalba (3C-MT)	8.47	419	0.53	26	21.00	82
Ghisalba (3C-BI)	5.03	336	0.31	21	19.00	86
Poncarale (1C)	34.52	643	2.15	41	28.00	70
Poncarale (2C-BI)	75.88	1006	4.74	63	63.00	53

541 *5.2 Positions and speeds validation*

542 Since the distances between the RTK-GPS data and the VeTRA probe vehicle obtained data are not

543 Gaussian distributed, the MOTP index (Bernardin and Stiefelhagen, 2008) is split into three other

544 indexes – the median, median of absolute deviations (MAD), and inter-quartile range (IQR) (Table 4).

545 The results are available for the six different analyses carried out on the three roundabouts and the

546 different strategies of image processing. Furthermore, Table 4 lists the average and the standard

547 deviation of the speed differences recorded by both the on-board RTK-GPS system and by the

548 tracking process, for the same combination of roundabout and image processing strategies.

549 The results show that differences in positions and speed occur when different configurations and

550 processing strategies are adopted. The best performances in terms of tracking were observed in the

551 following cases: single camera configuration (Biella), two cameras with image blending (2C-BI) and

552 merged trajectory (2C-MT) strategy (Poncarale). Greater distances between tracked points were

553 measured when configuration #2 of Fig. 4 with three central cameras was adopted, and in the case of

554 the survey carried out at Poncarale, where only one camera was used to analyse vehicle movements

555 at a roundabout with the largest diameter (70 m) between the three here investigated.

556 As regards speeds, the best results in terms of average and standard deviation were noted in the

557 Biella survey, while the worst performances were those in the Poncarale survey in which the image

560
561

Table 4 Distribution of errors in distance and speed difference between VeTRA and RTK-GPS data.

Roundabout	Distance (m)			Speed difference (km/h)	
	Median	MAD	IQR	Average	Standard deviation
Biella (1C)	0.375	0.179	0.399	0.11	2.71
Ghisalba (3C-MT)	0.651	0.457	0.863	0.12	7.31
Ghisalba (3C-BI)	0.272	0.743	0.619	3.06	8.87
Poncarale (1C)	0.576	0.250	0.576	11.46	23.66
Poncarale (2C-MT)	0.383	0.191	0.436	1.06	8.64
Poncarale (2C-BI)	0.384	0.173	0.397	7.58	18.71

562

563 In the case of Poncarale with the strategy 2C-MT, data analysis was limited to speed analysis and

564 not extended to the whole set of analyses due to difficulties in building the whole trajectory. In too

565 many cases, the continuity of the trajectory curve was not achieved.

566 *5.3 Tortuosity and speeds analysis*

567 An analysis of tortuosity and related speeds was performed on the class of light vehicles only. For

568 each trajectory and at each point (i), VeTRA derives the two tortuosity indexes and local speeds from

569 the recorded positions and times when the centre of the vehicle occupies the points $i+1$, i and i-1. All

570 the trajectories are grouped under the same O/D maneuver and the software can elaborate the

571 requested statistical output selected by the operator.

572 Table 5 contains the synthesis of the 15th percentile of the two tortuosity indexes ($T_{1,15}$ and $T_{2,15}$)

573 calculated for those parts of the trajectories including the entry and exit gates of the roundabouts, and

574 the 85th percentile of corresponding speeds at: (1) the entry gate ($V_{1,85}$), (2) the midpoint of the

575 trajectory inside the circulatory roadway ($V_{2,85}$), and (3) the exit gate ($V_{3,85}$) as indicated in Fig. 1. The

576 data in Table 5 was evaluated on the base of 2208 measurements of light vehicles operating in free-

577 flow conditions. According to Fig. 6(a), in the case of Ghisalba, only three maneuvers were completely

578 measured; in the case of Biella and Poncarale, the number of performance measures per O/D was

579 lower than sixteen (four origins per four destinations) since the number of vehicles recorded for certain

580 maneuvers (typically the U-turn) was too low.

581
582

Table 5 Filtered trajectory data for 15th percentile of tortuosity and 85th percentile of operating speed.

Biella 1C	2-3	Right turn	20	0.00124	0.0311	32.27	34.07	39.37
	2-5	Crossing	185	0.00015	0.0096	33.88	39.00	44.11
	4-1	Left turn	21	0.00200	0.0372	29.58	27.75	40.55
	4-5	Right turn	50	0.00129	0.0330	29.33	30.44	33.62
	4-7	Crossing	73	0.00069	0.0216	30.61	36.09	41.38
	6-1	Crossing	185	0.00094	0.0255	32.71	33.43	42.68
	6-3	Left turn	42	0.00207	0.0383	33.70	29.52	42.43
	6-7	Right turn	83	0.00064	0.0218	34.63	34.66	37.27
	8-1	Right turn	20	0.00054	0.0207	31.89	33.08	37.88
	8-3	Crossing	72	0.00041	0.0163	36.11	35.51	44.56
	8-5	Left turn	97	0.00179	0.0336	33.56	27.81	39.64
Ghisalba 3C-BI	2-3	Right turn	33	0.00047	0.0204	34.15	36.27	35.52
	2-5	Crossing	364	0.00070	0.0224	36.70	35.80	40.07
	4-5	Right turn	9	0.00032	0.0168	35.25	38.66	40.76
Ghisalba 3C-MT	2-3	Right turn	33	0.00050	0.0203	30.70	32.90	33.67
	2-5	Crossing	364	0.00067	0.0221	36.41	35.83	40.22
	4-5	Right turn	9	0.00037	0.0182	31.57	34.61	39.18
Poncarale 2C-BI	4-1	Left turn	42	0.00077	0.0241	43.60	37.70	47.02
	4-7	Crossing	183	0.00035	0.0152	40.26	39.59	46.31
	2-3	Right turn	22	0.00100	0.0298	32.43	32.71	38.91
	2-7	Left turn	28	0.00075	0.0233	34.67	35.47	44.92
	8-3	Crossing	226	0.00048	0.0177	37.76	38.03	45.25
	8-1	Right turn	47	0.00007	0.0065	39.09	44.88	49.48

583
584   The 85th percentile of speed distribution is widely considered in the geometric design of highways.

585   It is compared with the design speed to assess speed consistency between the hypothesis of

586   designer and driver behaviour. It reflects the movement of isolated vehicles (i.e., free-flow conditions),

587   and separates the population of prudent drivers from the group of more aggressive ones (Yasser and

588   Mohamed, 2011).

589   The choice of the two percentiles is based on the supposition that aggressive drivers, whose

590   speeds exceed the 85th percentile, tend to follow the fastest path that should be characterized by the

591   lowest tortuosity (as also suggested in Rodegerdts et al., 2007, 2010). The authors associated the

592   15th percentile of tortuosity indexes with the fastest path so as to establish correlations between

593   trajectory and speeds.

594   When the analysis is confined to a part of the speed data, the most significant relationships

596 middle point of trajectories ($V_{2,85}$) and the 15th percentile of the two tortuosity indexes $T_{1,15}$ and $T_{2,15}$.

597 The results are reported in Figs. 7 and 8, and demonstrate that $T_{2,15}$ rather than $T_{1,15}$ has a rather good

598 correlation to $V_{2,85}$ as confirmed by the statistics of the two models summarized in Table 6.

599 Figs. 7 and 8 also report the data generated with the MT strategy in the case of the Ghisalba

600 roundabout. These data are more dispersed when compared to the corresponding data derived with

601 the BI strategy, and, as a consequence, they were not taken into account in the exponential model

602 which was plotted in both figures, and which exhibited the highest coefficient of determination for both

603 tortuosity indexes.

604 Very low correlation values were found between the 85th percentile of entry (V_1) and exit (V_3)

605 speeds. This may be attributed to the fact that the entry speed largely depends on driver behaviour in

606 the approaching leg, while the exiting speed depends more on the specific shape of curbs around the
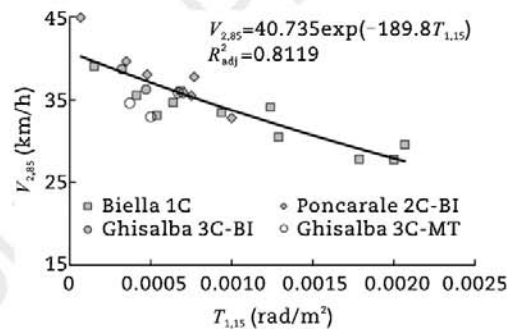
607 exit lane.

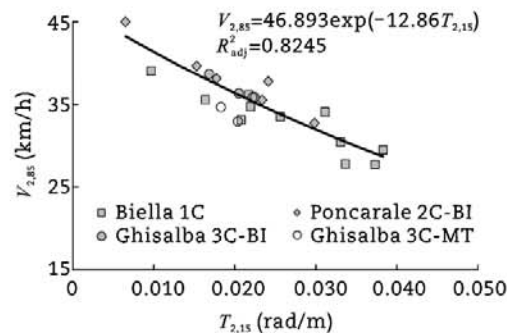**Fig. 7** Relationship between $V_{2,85}$ and $T_{1,15}$ index.

Fig. 8 Relationship between $V_{2,85}$ and $T_{2,15}$ index.

Table 6 Output of statistics for model reported in Figs. 7 and 8.

	Column A	Column B
R^2	0.8218	0.8337
R^2 adjusted	0.8119	0.8245
Standard error	0.0520	0.0510
F value	83.0259	90.2644
	(F critical = 2.17, p = 0.05)	(F critical = 2.17, p = 0.05)
p value Intercept	1.27×10^{-30}	2.90×10^{-27}
Variable	3.66×10^{-8}	1.95×10^{-8}

618

619   It must be stressed that we limited the study of correlation between speed and tortuosity only to
620   three points (entry, middle and exit) as reproduction of the approach proposed by Rodegerdts et al.
621   (2007).

622   *5.4   Acceleration analysis*

623   Table 7 shows the statistics for acceleration and deceleration measured on the circulatory roadway for
624   the Ghisalba and Poncarale roundabouts (trajectory data are the same of Table 5). It should be
625   highlighted once again that the data considered here pertain to vehicles that were not affected by
626   other vehicles when negotiating the roundabout, thus all the data can be considered to be that of
627   isolated vehicles and drivers affected by the roundabout geometrics only.

628   According to the speed variation model depicted in Fig. 1, the deceleration from sections 1 to 2 is
629   indicated as a_{12}, while the acceleration from the central point of the trajectory (section 2) to the exit
630   section (section 3) is indicated as a_{23}.

631
632   **Table 7** Statistics for vehicular acceleration and deceleration at the Ghisalba and Poncarale roundabouts.

Roundabout	Ghisalba 3C-BI				Poncarale 2C-BI					
	Right turn		Through		Right turn		Through		Left turn	
Acceleration	a_{12}	a_{23}	a_{12}	a_{23}	a_{12}	a_{23}	a_{12}	a_{23}	a_{12}	a_{23}
No. of objects	42	42	364	364	69	69	409	409	70	70
Mean (m/s^2)	−0.614	0.116	−0.063	0.409	−0.674	0.719	−0.264	0.468	−0.051	0.358
Standard deviation (m/s^2)	0.601	0.499	0.370	0.273	1.030	0.660	0.555	0.616	0.312	0.204
15th percentile (m/s^2)	−1.241	−0.556	−0.378	0.142	−1.724	0.117	−0.831	0.141	−0.371	0.205
85th percentile	−0.038	0.606	0.281	0.676	0.132	1.261	0.235	0.744	0.257	0.543

Min (m/s²)	−1.901	−0.721	−1.948	−0.793	−3.201	−1.474	−2.156	−0.832	−0.895	−0.518

633
634   Per each vehicle traversing the roundabout, these two values were computed with the following

635 equations.

$$a_{12} = (v_{22} - v_{12}) / (2d_{12}) \tag{10}$$

$$a_{23} = (v_{32} - v_{22}) / (2d_{23}) \tag{11}$$

638 where d_{12} and d_{23} have the same meaning of Eqs. (1) and (2). Data have also been distinguished for

639 left turn, right turn, and through movements.

640   The mean and the standard deviation of acceleration values indicate that entering vehicles in

641 deceleration (a_{12}) and exiting vehicles in acceleration (a_{23}) exhibit large variations as a result of the

642 roundabout layout and geometrics, and type of maneuvers. The 15th percentiles of deceleration (a_{12}),

643 listed in Table 7, are only higher in the case of right turn movements than the absolute value of 1.3

644 m/s² suggested in Rodegerdts et al. (2007), and reflect the behaviour of aggressive drivers. In all

645 other cases, the statistics for a_{12} indicate that lower values are observed.

646   Regarding the acceleration variable (a_{23}), a large difference is evident between the observed values

647 and the value of 2.3 m/s² proposed again in Rodegerdts et al. (2007), thus suggesting the need for an

648 extended investigation into a greater number of roundabout geometry types. In fact, the two

649 roundabouts considered here yield different results as a consequence of the significant difference in

650 their layout.

651 **6 Discussion**

652 The results illustrated in previous paragraphs outlined the strengths and weaknesses associated with

653 each set-up for the three different roundabouts considered in the investigation. In the three cases,

654 small camera oscillations, clouds, and flying objects (i.e., birds) affecting image quality were easily

655 identified and corrected.

656   On examination of the three configurations presented in Fig. 4, it is clear that the central position of

657 the video cameras facilitates a reduction in perspective distortion but, as in the case of Ghisalba

659   given the dimensions of the circulatory roadway. The blending of images becomes more complicated

660   with an increase in the number of video cameras installed at or around the roundabout. Moreover,

661   synchronization between cameras becomes crucial: with the loss of only one frame of a video camera

662   necessitating a challenging task of realignment between video frames.

663   Elevated vantage points on poles or buildings introduce high levels of distortion especially in the

664   case of heavy and long vehicles, as in the case of Poncarale (configuration #3 in Fig. 4 with three

665   cameras). Furthermore, the height of vantage points has a detrimental impact on image quality since

666   the cameras and their supports are exposed to stronger winds, which can produce oscillations that are

667   hard to correct during the image treatment phase. From an analysis of the data collected at the

668   Poncarale roundabout, it would appear that the merging of trajectories extracted from different images

669   (MT strategy) seems to be less effective than the blending images (BI) technique. In this case, the

670   only one for which this comparison has been made, the performance indicators associated with the

671   evaluation of the O/D matrix indicate a greater dispersion of data in the case of the merged trajectory

672   technique (Table 5).

673   Whereas the blending of images is essentially a straightforward task when video cameras have

674   viewing angles of less than 90°, it tends to prove problematic with wider angles (especially those

675   closer to 180°) as a consequence of the different perspective distortions of moving elements. Of the

676   three configurations considered in this research, the use of a single video camera mounted on a pole

677   located outside the roundabout, as in the case of Biella (with the camera located at the external side

678   of the circulatory roadway), would appear to offer the best compromise in terms of survey costs,

679   pre-processing work, and quality of results. However, this is not a definitive conclusion, since the

680   number of experiments carried out to date is not considered comprehensive from a technological point

681   of view. In this study, the authors focused primarily on a general evaluation of the methodology and

682   the estimation of technical problems to be solved for each specific configuration. In fact, while the

683   results here have been used to assess the survey methodology, they cannot be considered

684   statistically significant in terms of the performances of the investigated roundabouts or, indeed,

686   In all the three configurations depicted in Fig. 4, VeTRA has been able to collect spatial and

687   temporal data for a large number of points along each trajectory, thus deriving local speeds. The

688   authors decided to consider speeds at the entry gate, at the midpoint and at the exit of the roundabout

689   to compare results with those in Rodegerdts et al. (2007). Two different tortuosity indexes were

690   calculated for each trajectory by combining angular deviation and the distance between two

691   successive recorded points, and the radius of the local osculating circle in different ways.

692   As a result, some linear and exponential relationships between the 85th percentile of speeds and

693   the 15th percentile of tortuosity indexes have been derived. The observations confirm that an effective

694   speed control within the circulatory roadway is possible only when high horizontal curvatures of

695   vehicle paths (i.e., high values of tortuosity) are achieved as a consequence of the combination of the

696   geometric characteristics of roundabout elements.

697   The regression equations presented here were obtained from 2208 speed data (Table 5) of just

698   three roundabouts with each exhibiting a different geometry in terms of external and central island

699   diameters, circulatory roadway width, number and geometry of entry and exit lanes. The high

700   coefficient of determination of one of four proposed equations (R^2 = 0.8337 for the exponential

701   relationship between $V_{2,85}$ and the $T_{2,15}$) facilitates its use in the estimation of the circulating operating

702   speed ($V_{2,85}$) in the analysis and design of roundabouts.

703   Acceleration and deceleration values on the circulatory roadways exhibit large variations as a

704   consequence of roundabout layout and geometrics, maneuver type, and driving attitudes and styles.

705   In light of the observation data, the suggested values of −1.3 m/s^2 in deceleration and 2.1 m/s^2 in

706   acceleration included in the NCHRP Reports 572 and 672 (Rodegerdts et al., 2007, 2010) seem to be

707   questionable, thus new research is necessary to obtain better design-operating speed and

708   acceleration distribution on the circulatory roadway. This paper has demonstrated that image analysis

709   has the potential to achieve such objectives.

710

711

713 **7 Conclusions**

714 The paper presents the results of several activities undertaken involving extensive use of the VeTRA

715 software and acquisition tools, which the authors developed for the specific purpose of carrying out

716 operational analyses of roundabouts through the use of video-tracking technology.

717 At present, the comprehensive gathering of operational data at roundabouts necessitates the use of

718 non-integrated acquisition systems and prolonged data analysis times. Since 2010, the authors have

719 worked on the development of an integrated system (specifically designed for roundabouts)

720 composed of a hardware system for data acquisition and collection, and software for data analysis.

721 The system and some data analysis have already been presented in previous referenced works

722 (Mussone et al., 2011, 2013), in which the system included one video camera only.

723 In this paper, the authors focused their attention on an extended use of the software with the aims

724 of solving issues related to the survey configuration used with more than one video camera and their

725 positioning inside or around the roundabout, and improving the tracking system of vehicles and

726 deriving the O/D matrix and trajectories (i.e., position and time of tracked vehicles).

727 Two possible strategies consisting in (a) the merging of trajectories extracted from each separate

728 video, and (b) the image blending from different video cameras before extracting trajectories were

729 investigated. Results suggest that the second is more effective than the first one. Furthermore, of the

730 three configurations considered, the one consisting in a single video camera mounted on a pole

731 outside the roundabout appeared to be the optimal in terms of costs, processing work, and quality of

732 results. However, this solution may imply large perspective distortion of the tracked vehicles in

733 locations far from the camera, especially in case of roundabout with large diameters. To limit

734 perspective distortion, the vantage point must be raised up as much as possible.

735 From the data collected from case studies, one further result concerns the correlation between

736 speed and tortuosity of vehicle trajectories, which could be used by designers in the estimation of

737 vehicle performance when negotiating a roundabout. This result emphasizes the tremendous potential

738 of the image analysis in capturing position and kinematic of vehicles, and opens up to further studies

740 In conclusion, previous works by the authors, together with the results reported in this paper, testify

741 to the fact that the video survey system and the processing code are both robust and reliable. As

742 documented in this paper, the authors are aware that further work is necessary to improve the

743 performance of the tracking system of VeTRA in all possible set-up configurations.

744 With this objective in mind, a new version of the software is under development. It will include a set

745 of 3D models of vehicles that differ in terms of dimensions and that can be associated with each blob.

746 In this way, trajectories will be derived with reference to the geometric centre of the model rather than

747 to the centre of the blob. This approach, already adopted by some authors but in different road

748 scenarios (Kim et al., 2005; Koller et al., 1993; Messelodi et al., 2005), can lead to better vehicle

749 recognition, which is considerable when high perspective distortions are present (like in Poncarale),

750 together with even more precise localization and tracking. The authors are confident that the use of

751 vehicle models will reduce the negative effect of video camera oscillations and will enable the

752 separation of the shadows (of vehicles) from the actual vehicles in blobs, thus reducing the impact of

753 shadows on the quality of collected data. Finally, to extend the possibility of data collection to night-

754 time conditions, new research will also be carried out assessing how to use videos from thermal

755 and/or infra-red video cameras.

756 **Conflict of interest**

757 The authors do not have any conflict of interest with other entities or researchers.

758 **References**

759 Ahac, S., Džambas, T., Dragčević, V., 2016. Review of fastest path procedures for single-lane

760 roundabouts. In: The 4th International Conference on Road and Rail Infrastructure (CETRA),

761 Sibenik, 2016.

762 Alhajyaseen, W.K.M., Asano, M., Nakamura, H., et al., 2013. Stochastic approach for modeling the

763 effects of intersection geometry on turning vehicle paths. Transportation Research Part C:

765 Apeltauer, J., Babinec, A., Herman, D., et al., 2015. Automatic vehicle trajectory extraction for traffic

766   analysis from aerial video data. The International Archives of Photogrammetry, Remote Sensing

767   and Spatial Information Sciences 40(3), 9.

768 Autodesk, 2018. Civil 3D: Civil Infrastructure Design and Documentation Software. Available at:

769   https://www.autodesk.com/products/civil-3d/overview (Accessed 10 September 2019).

770 Bernardin, K., Stiefelhagen, R., 2008. Evaluating multiple object tracking performance: the CLEAR

771   MOT metrics. EURASIP Journal on Image and Video Processing 2008, 1-10.

772 Beymer, D., McLauchlan, P., Coifman, B., et al., 1997. A real-time computer vision system for

773   measuring traffic parameters. In: IEEE Computer Society Conference on Computer Vision and

774   Pattern Recognition, San Juan, 1997.

775 Curti, V., Marescotti, L., Mussone, L., 2008. Roundabouts: Design and Evaluations of Roundabout

776   Intersections, fourth ed. Maggioli, Ravenna.

777 Datondji, S.R.E., Dupuis, Y., Subirats, P., et al., 2016. A survey of vision-based traffic monitoring of

778   road intersections. IEEE Transactions on Intelligent Transportation Systems 17(10), 2681-2698.

779 Dinh, H., Tang, H., 2017. A video processing system for automated traffic data collection of gap size

780   for roundabouts. In: IEEE 30th Canadian Conference on Electrical and Computer Engineering,

781   Windsor, 2017.

782 Fernandes, P., Salamati, K., Rouphail, N.M., et al., 2015. Identification of emission hotspots in

783   roundabouts corridors. Transportation Research Part D: Transport and Environment 37, 48-64.

784 Grenard, J.L., Wei, T., 2012. Traffic Counting at Roundabouts Using Video Technology: A

785   Practitioner's View–White Paper. Available at: http://miovision.com/white-papers-research-reports/

786   (Accessed 2 March 2014).

787 Guido, G., Gallelli, V., Rogano, D., et al., 2016. Evaluating the accuracy of vehicle tracking data

788   obtained from unmanned aerial vehicles. International Journal of Transportation Science and

789   Technology 5(3), 136-151.

790 Kim, Z.W., Gomes, G., Hranac, R., et al., 2005. A machine vision system for generating vehicle

793 Koller, D., Daniilidis, K., Nagel, H.H., 1993. Model-based object tracking in monocular image
794   sequences of road traffic scenes. International Journal of Computer Vision 10(3), 257–281.

795 Messelodi, S., Modena, C.M., Zanin, M., 2005. A computer vision system for the detection and
796   classification of vehicles at urban road intersections. Pattern Analysis and Applications 8(1-2), 17-
797   31.

798 Migliore, D.A., Matteucci, M., Naccari, M., 2006. A revaluation of frame difference in fast and robust
799   motion detection. In: The 4th ACM International Workshop on Video Surveillance and Sensor
800   Networks, Santa Barbara, 2006.

801 Mussone, L., 2013. The analysis of roundabouts through visibility. Procedia – Social and Behavioral
802   Sciences 87, 250-268.

803 Mussone, L., Matteucci, M., Bassani, M., et al., 2011. Traffic analysis in roundabout intersections by
804   image processing. In: The 18th International Federation of Automatic Control (IFAC) World
805   Congress, Milano, 2011.

806 Mussone, L., Matteucci, M., Bassani, M., et al., 2013. An innovative method for the analysis of vehicle
807   movements in roundabouts based on image processing. Journal of Advanced Transportation
808   47(6), 581–594.

809 Oh, J., Min, J., Heo, B., 2012. Development of an integrated system based vehicle tracking algorithm
810   with shadow removal and occlusion handling methods. Journal of Advanced Transportation 46(2),
811   139–150.

812 Perco, P., Marchionna, A., Falconetti, N., 2012. Prediction of the operating speed profile approaching
813   and departing intersections. Journal of Transportation Engineering 138(12), 1476-1483.

814 Robinson, B.W., Rodegerdts, L., Scarbrough, W., et al., 2000. Roundabouts: an Informational Guide.
815   FHWA-RD-00-067. Federal Highway Administration, U.S. Department of Transportation,
816   Washington DC.

817 Rodegerdts, L., Blogg, M., Wemple, E., et al., 2006. Appendixes to NCHRP Report 572: Roundabouts
818   in the United States. NCHRP Web-Only Document 94. Transportation Research Board, National

820 Rodegerdts, L., Blogg, M., Wemple, E., et al., 2007. Roundabouts in the United States. NCHRP
821   Report 572. Transportation Research Board, National Research Council, Washington DC.

822 Rodegerdts, L., Bansen, J., Tiesler, C., et al., 2010. Roundabouts: an Informational Guide. NCHRP
823   Report 672. Transportation Research Board, National Research Council, Washington DC.

824 Rodegerdts, L., Jenior, P.M., Bugg, Z.H., et al., 2014. Evaluating the Performance of Corridors with
825   Roundabouts. NCHRP Report 772. Transportation Research Board, Washington DC.

826 Sacchi, E., Bassani, M., Persaud, B., 2011. Comparison of safety performance models for urban
827   roundabouts in italy and other countries. Transportation Research Record 2265, 253-259.

828 Sakshaug, L., Laureshyn, A., Svensson Å., et al., 2010. Cyclists in roundabouts – different design
829   solutions. Accident Analysis & Prevention 42(4), 1338-1351.

830 Salamati, K., Coelho, M.C., Fernandes, P., et al., 2013. Emissions estimation at multilane
831   roundabouts: effects of movement and approach lane. Transportation Research Record 2389, 12-
832   21.

833 St-Aubin, P., Saunier, N., Miranda-Moreno, L.F., 2013. Detailed driver behaviour analysis and
834   trajectory interpretation at roundabouts using computer vision data. Transportation Research
835   Record 2389, 65-77.

836 Šurdonja, S., Dragčević, V., Deluka-Tibljaš, A., 2018. Analyses of maximum-speed path definition at
837   single-lane roundabouts. Journal of Traffic and Transportation Engineering (English Edition) 5(2),
838   83-95.

839 Suzuki, K., Nakamura, H., 2006. TrafficAnalyzer – the integrated video image processing system for
840   traffic flow analysis. In: The 13th Intelligent Transportation Systems World Congress, London,
841   2006.

842 Transoftsolutions, 2018. TORUS Roundabouts: Roundabout Design Software. Available at:
843   https://www.transoftsolutions.com/road-design/torus-roundabouts/ (Accessed 2 January 2019).

844 Wei, H., Feng, C., Meyer, E., et al., 2005. Video-capture-based approach to extract multiple vehicular
845   trajectory data for traffic modeling. Journal of Transportation Engineering 131(7), 496-505.

848   Zaki, M.H., Sayed, T., Cheung, A., 2013. Computer vision techniques for the automated collection of

849   cyclist data. Transportation Research Record 2387, 10-19.

850

851

852   Marco Bassani, PhD, is an associate professor in roads, railways and airport engineering at the

853   Politecnico di Torino (Italy) where he teaches "Design of Transportation Infrastructures". In 2014,

854   he was a visiting professor at the University of Maryland (College Park, US). His main research

855   interests and publications are related to the use of alternative materials, advanced geometric

856   design of roads, driving simulation, and road safety. Since 2016, he is in the editorial board of

857   Transportation Letters: The International Journal of Transportation Research.

858

859

860   Lorenzo Mussone held a master degree in electronic engineering in 1982 and a PhD in

861   transportation engineering in 1995. Since 2011, he is an associate professor at Politecnico di

862   Milano. The main scientific activities concern modelling by different techniques: partial derivative

863   macroscopic equations, microscopic simulation, neural networks, swarm intelligence and graph

864   theory, applied to road accident data analysis, vehicular flow control, capacity of complex railway

865   systems, driver behaviour study, roundabouts design, transportation network analysis, and ITS

866   applications. He is in the panel of reviewers of many transportation journals. Since 2005, he is in

867   the editorial board of Accident Analysis & Prevention journal and Transportation Research

868   Interdisciplinary Perspectives.

Conflict of Interest and Authorship Conformation Form

Please check the following as appropriate:

X   All authors have participated in (a) conception and design, or analysis and
     interpretation of the data; (b) drafting the article or revising it critically for
     important intellectual content; and (c) approval of the final version.

X   This manuscript has not been submitted to, nor is under review at, another
     journal or other publishing venue.

X   The authors have no affiliation with any organization with a direct or indirect
     financial interest in the subject matter discussed in the manuscript

o   The following authors have affiliations with organizations with direct or
     indirect financial interest in the subject matter discussed in the manuscript:

Author's name	Affiliation
Lorenzo Mussone	Politecnico di Milano, Italy
Marco Bassani	Politecnico di Torino, Italy